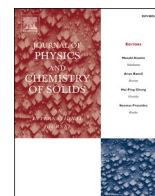




Contents lists available at ScienceDirect

## Journal of Physics and Chemistry of Solids

journal homepage: [www.elsevier.com/locate/jpcs](http://www.elsevier.com/locate/jpcs)

# Design and synthesis of nickel tetra-2,3-pyridiniumporphyrazinato trinitromethanide as an influential catalyst and its application in the synthesis of 1,2,4-triazolo based compounds

Mohammad Dashteh<sup>a</sup>, Saeed Baghery<sup>a,\*</sup>, Mohammad Ali Zolfigol<sup>a,\*\*</sup>, Ardeshir Khazaei<sup>a,\*\*\*</sup>, Sajjad Makhdoomi<sup>b</sup>, Maliheh Safaiee<sup>c</sup>, Jamshid Rakhtshah<sup>d,\*\*\*\*</sup>, Yadollah Bayat<sup>e</sup>, Asiye Asgari<sup>e</sup>

<sup>a</sup> Department of Organic Chemistry, Faculty of Chemistry, Bu-Ali Sina University, Hamedan, 6517838683, Iran

<sup>b</sup> Department of Pharmacology and Toxicology, School of Pharmacy, Hamedan University of Medicinal Science, Hamedan, Iran

<sup>c</sup> Department of Medicinal Plants Production, University of Nahavand, Nahavand, 6593139565, Iran

<sup>d</sup> Department of Inorganic Chemistry, Faculty of Chemistry, University of Tabriz, Tabriz, Iran

<sup>e</sup> Faculty of Chemistry and Chemical Engineering, Malek Ashtar University of Technology, Tehran, Iran

## ARTICLE INFO

## Keywords:

Nickel tetra-2,3-pyridiniumporphyrazinato trinitromethanide [Ni(TPPAH)][C(NO<sub>2</sub>)<sub>3</sub>]<sub>4</sub>  
Solvent-free condition  
[1,2,4]Triazolo[1,5-*b*]pyrimidines  
[1,2,4]Triazolo[5,1-*b*]quinazolines

## ABSTRACT

The facile and benign syntheses of [1,2,4]triazolo[5,1-*b*]quinazolines and [1,2,4]triazolo[1,5-*b*]pyrimidines were studied using novel nickel tetra-2,3-pyridiniumporphyrazinato trinitromethanide [Ni(TPPAH)][C(NO<sub>2</sub>)<sub>3</sub>]<sub>4</sub> as an efficient catalyst. The desired products were synthesized under solvent-free conditions using 10 mg of [Ni(TPPAH)][C(NO<sub>2</sub>)<sub>3</sub>]<sub>4</sub> as a catalyst at 80 °C. The morphology and structure of [Ni(TPPAH)][C(NO<sub>2</sub>)<sub>3</sub>]<sub>4</sub> were studied and characterized using several techniques. The products had good to excellent yields with short reaction times. The presented catalyst was simply recovered and reused. Some of the obtained products (10 items) are reported for the first time.

## 1. Introduction

The production of numerous bonds in a one-step process has been developed as a significant methodology for organic synthesis [1,2]. Multi-component reactions (MCRs) have been considered to synthesize biologically active compounds and have become a major area of study in organic chemistry and pharmacology [3,4]. The chief advantages of MCRs are high bond-forming efficacy, lower cost, easy work-up, energy saving and hence decreased waste generation by developing green routes [5,6].

Nitrogen-including heterocyclic skeletons have major roles in several types of chemical compounds. Among these compounds, quinazolines and pyrimidines are advantageous as building blocks and so have been investigated widely due to their outstanding pharmacological activities [7–11]. Additionally, the triazoles are major fundamental motifs in

chemistry and medicinal chemistry and are used to establish numerous biologically active compounds [12–14]. These compounds have various biological properties, for instance therapeutic potentiality [15], anti-convulsant [16], cytotoxicity [17], antidiabetic [18], anti-tumor [19], antiviral [20] and cardiovascular activities [21]. Triazolo-quinazolines and -pyrimidines have been synthesized using numerous methods and reagents including nano *n*-propylsulfonated  $\gamma$ -Al<sub>2</sub>O<sub>3</sub> [22], sulfamic acid [23], Lawesson's reagent [24] and Nafion-H [25].

Phthalocyanines (Pcs) of transition metals are noteworthy as potential oxidation catalysts due to their low-cost and simple synthesis on a large scale and their thermal stability [26]. The Pcs are one of the important groups of macrocycles and are broadly applied for various purposes such as catalytic systems, Langmuir–Blodgett films, chemical sensors, molecular metals and liquid crystals [27,28]. Metal Pcs have a planar structure and are aromatic complexes of porphyrins [29,30].

\* Corresponding authors.

\*\* Corresponding author.

\*\*\* Corresponding author.

\*\*\*\* Corresponding author.

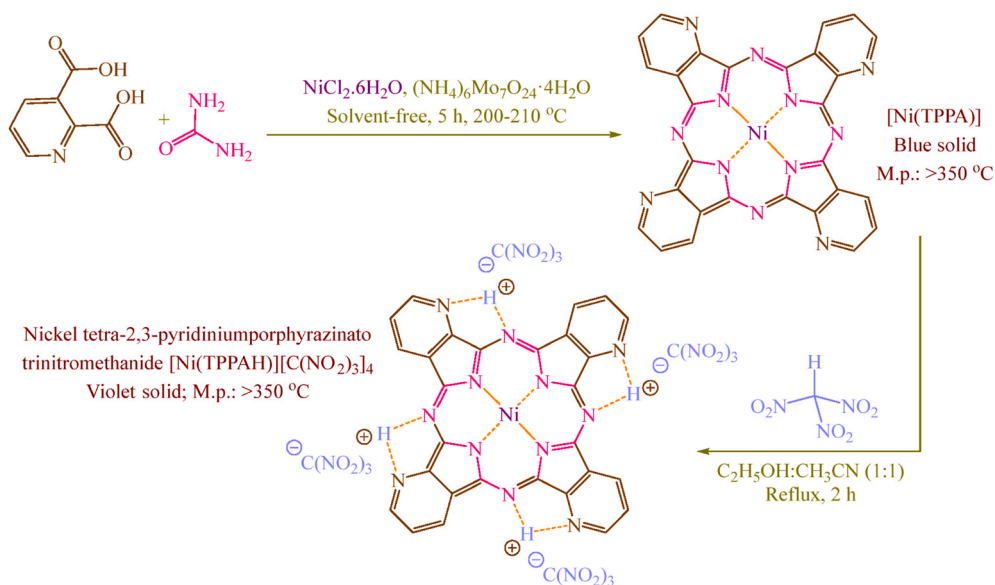
E-mail addresses: [saadybaghery@yahoo.com](mailto:saadybaghery@yahoo.com) (S. Baghery), [zolfi@basu.ac.ir](mailto:zolfi@basu.ac.ir), [mzolfigol@yahoo.com](mailto:mzolfigol@yahoo.com) (M.A. Zolfigol), [Khazaei\\_1326@yahoo.com](mailto:Khazaei_1326@yahoo.com) (A. Khazaei), [j.rakhtshah@tabrizu.ac.ir](mailto:j.rakhtshah@tabrizu.ac.ir) (J. Rakhtshah).

<https://doi.org/10.1016/j.jpcs.2021.110322>

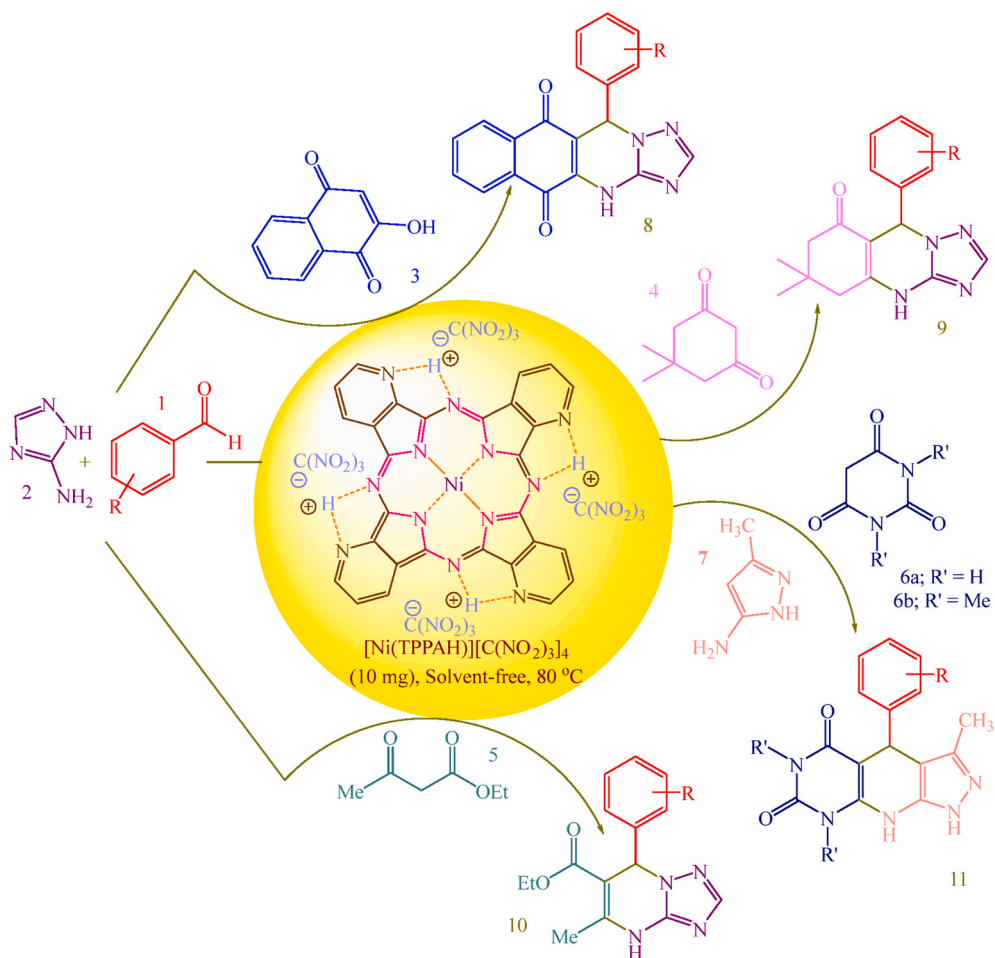
Received 31 December 2020; Received in revised form 29 July 2021; Accepted 9 August 2021

Available online 13 August 2021

0022-3697/© 2021 Elsevier Ltd. All rights reserved.



**Scheme 1.** Synthesis of nickel tetra-2,3-pyridiniumporphyrinato trinitromethanide  $[\text{Ni}(\text{TPPAH})][\text{C}(\text{NO}_2)_3]_4$ .



**Scheme 2.** Synthesis of [1,2,4]triazolo[5,1-*b*]quinazolines and [1,2,4]triazolo[1,5-*b*]pyrimidines using  $[\text{Ni}(\text{TPPAH})][\text{C}(\text{NO}_2)_3]_4$ .

As part of our consideration of the chemistry of Pcs-based catalysts [31,32], herein, we report an investigation on three-component synthesis of [1,2,4]triazolo[5,1-*b*]quinazolines and [1,2,4]triazolo[1,5-*b*]pyrimidines catalyzed by novel nickel tetra-2,

3-pyridiniumporphyrinato trinitromethanide  $[\text{Ni}(\text{TPPAH})][\text{C}(\text{NO}_2)_3]_4$  (Schemes 1 and 2). Some of the obtained products (10 items) are reported for the first time, and are characterized by several analyses including melting point, Fourier-transform infrared (FT-IR)

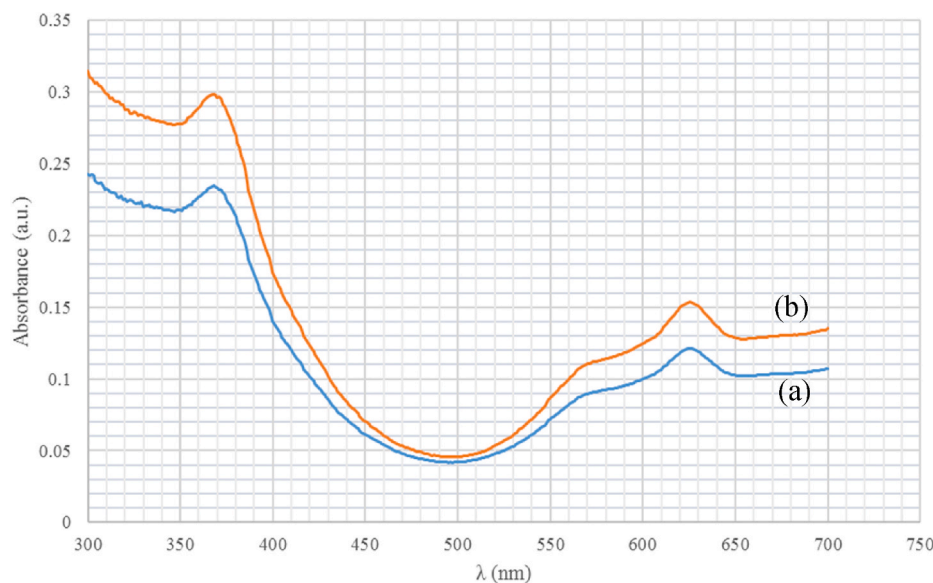


Fig. 1. UV-Vis spectra of (a) [Ni(TPPA)] and (b) [(OH)<sub>2</sub>Ni(TPPAH)][C(NO<sub>2</sub>)<sub>3</sub>]<sub>4</sub>.

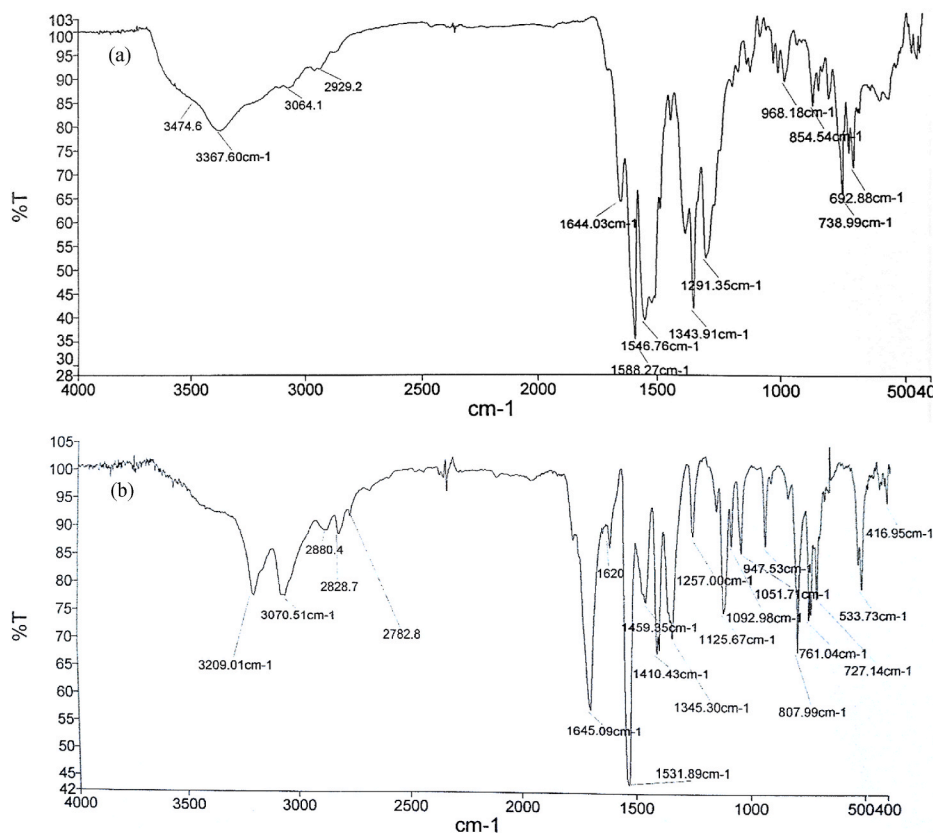


Fig. 2. FT-IR spectra of (a) [Ni(TPPA)] and (b) [(OH)<sub>2</sub>Ni(TPPAH)][C(NO<sub>2</sub>)<sub>3</sub>]<sub>4</sub>.

spectroscopy, <sup>1</sup>H nuclear magnetic resonance (NMR), <sup>13</sup>C NMR and elemental (CHN) analysis.

## 2. Experimental

### 2.1. General procedure for synthesis of [Ni(TPPA)]

The [Ni(TPPA)] was synthesized and purified based on reported procedures [33]. The general procedure follows: urea (6.5 g, 0.108 mol),

ammonium molybdate tetrahydrate [(NH<sub>4</sub>)<sub>6</sub>Mo<sub>7</sub>O<sub>24</sub>·4H<sub>2</sub>O] (0.046 g, 0.02 mol), 2,3-pyridine-dicarboxylic acid (1.0 g, 0.006 mol) and nickel (II) chloride hexahydrate [NiCl<sub>2</sub>·6H<sub>2</sub>O] (0.2 g, 0.0008 mol) were ground together to produce a homogenous mixture. The reaction mixture was refluxed in 1,2,4-trichlorobenzene (40 mL) at 160 °C for 5 h. Then, the mixture was allowed to cool to room temperature over 5 h. A crude blue solid was obtained and washed three times with warm water. Then the solid was washed with warm aqueous NaOH solution (5% w/v), warm water, warm diluted aqueous hydrochloric acid (2.5% v/v) and warm

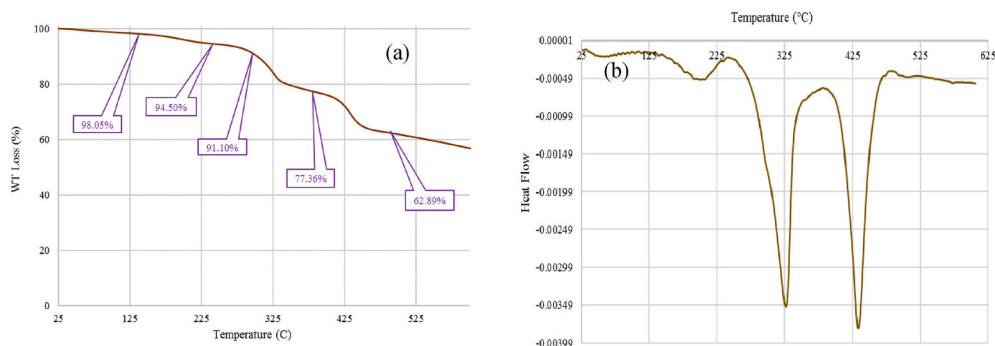


Fig. 3. (a) TGA and (b) DTA of  $[\text{Ni}(\text{TPPAH})][\text{C}(\text{NO}_2)_3]_4$ .

Table 1

Elemental analysis of (a)  $[\text{Ni}(\text{TPPA})]$  and (b)  $[\text{Ni}(\text{TPPAH})][\text{C}(\text{NO}_2)_3]_4$ .

Element		C	H	N
Wt.% (a)	Experimental	52.44	2.51	25.62
	Computational	55.21	2.32	27.59
Wt.% (b)	Experimental	32.10	1.75	27.97
	Computational	31.68	1.50	27.71

water consecutively. The obtained crude product was dried at 100 °C under vacuum and purified by dissolving in concentrated sulfuric acid and pouring the solution into ice-water. The precipitated product was collected by centrifugation (ca. 200 rpm/10 min) and transferred to a fine sintered glass funnel where the mass was washed with hot water, a warm aqueous sodium carbonate solution and warm water consecutively. The  $[\text{Ni}(\text{TPPA})]$  (isolated yield 41%, 3.176 g) was dried at 100 °C

under vacuum (Scheme 1).

## 2.2. General procedure for synthesis of $[\text{Ni}(\text{TPPAH})][\text{C}(\text{NO}_2)_3]_4$

To a round-bottomed flask (50 mL) including a solution of  $[\text{Ni}(\text{TPPA})]$  (3.176 g) in  $\text{C}_2\text{H}_5\text{OH}:\text{CH}_3\text{CN}$  (1:1; 4 mL), trinitromethane (4.0 mmol; 0.604 g; 0.411 mL) was added using a dropper over a period of 60 min while stirring and cooling to keep the temperature at 0–5 °C (caution: trinitromethane should be added with extreme caution due to its energetic character). Then, the reaction mixture was stirred for a further 120 min under reflux condition. The violet solid product  $[\text{Ni}(\text{TPPAH})][\text{C}(\text{NO}_2)_3]_4$  was washed three times with diethyl ether, dichloromethane and then dried under vacuum (isolated yield 59%, 2.230 g) (Scheme 1).

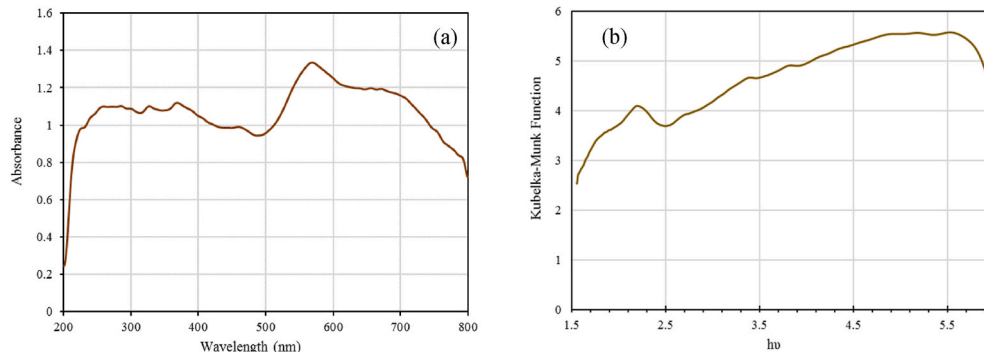


Fig. 4. (a) DRS analysis and (b) Kubelka–Munk function of  $[\text{Ni}(\text{TPPAH})][\text{C}(\text{NO}_2)_3]_4$ .

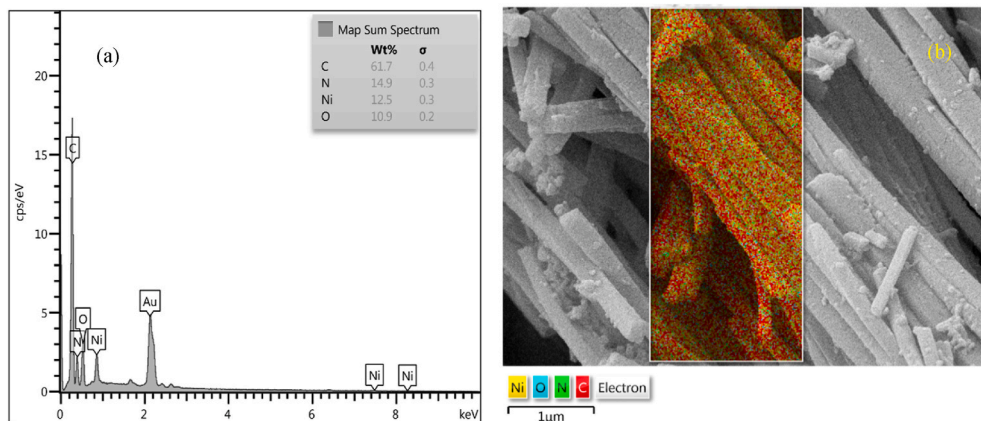


Fig. 5. (a) EDX analysis and (b) SEM coupled EDX (SEM mapping) of  $[\text{Ni}(\text{TPPAH})][\text{C}(\text{NO}_2)_3]_4$ .

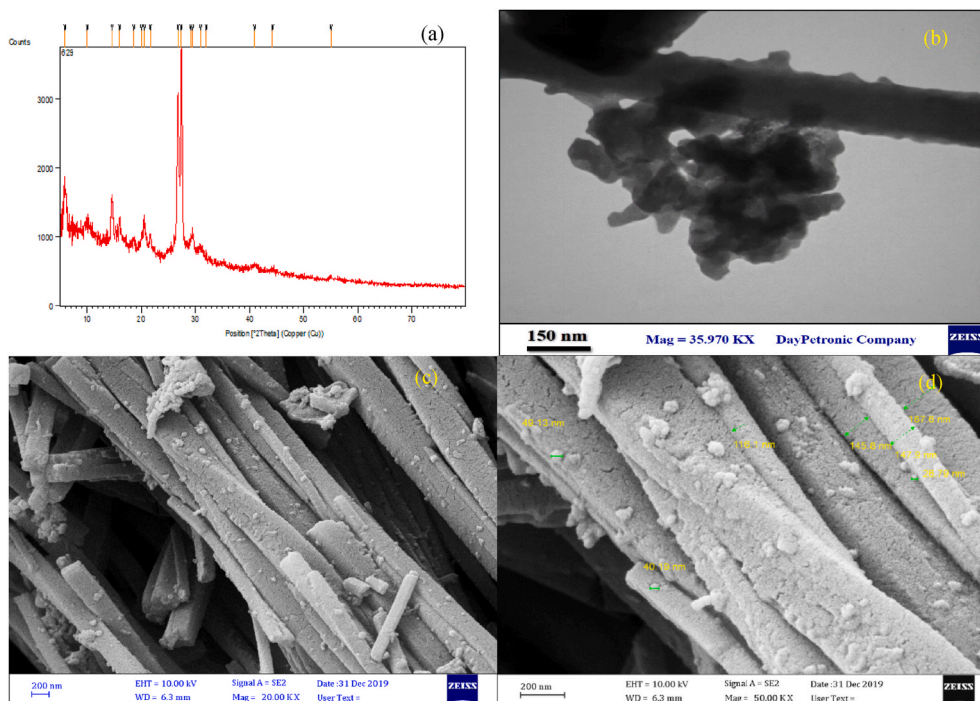
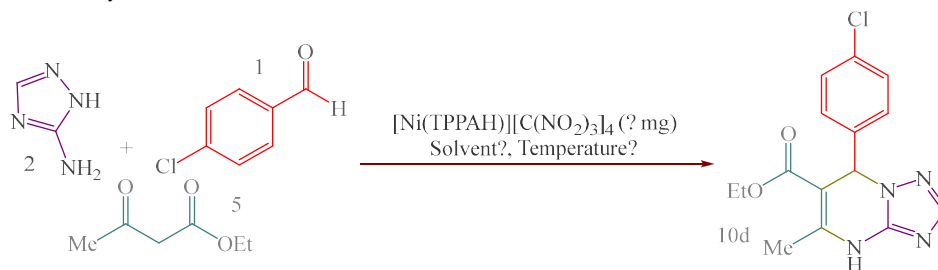


Fig. 6. (a) XRD pattern, (b) TEM and (c and d) SEM of  $[\text{Ni}(\text{TPPAH})][\text{C}(\text{NO}_2)_3]_4$ .

Table 2

Optimization reaction conditions for synthesis of **10d**.<sup>a</sup>



Entry	Solvent	Catalyst loading (mg)	Temperature (°C)	Time (min)	Yield <sup>b</sup> (%)
1	–	–	80	120	–
2	H <sub>2</sub> O	10	80	20	70
3	C <sub>2</sub> H <sub>5</sub> OH	10	Reflux	15	76
4	EtOAc	10	Reflux	60	–
5	CH <sub>3</sub> CN	10	Reflux	90	–
6	DMF	10	80	40	34
7	<i>n</i> -Hexane	10	Reflux	120	–
8	PEG	10	80	45	65
9	–	10	80	10	87
10	–	15	80	10	79
11	–	20	80	5	80
12	–	5	80	25	51
13	–	10	r.t.	120	–
14	–	10	50	30	Trace
15	–	10	100	15	80

<sup>a</sup> Reaction conditions: 4-chlorobenzaldehyde (1.0 mmol, 0.140 g), 3-amino-1,2,4-triazole (1.0 mmol, 0.084 g, 0.014 mL), ethyl acetoacetate (1.0 mmol, 0.130 g, 0.008 mL).

<sup>b</sup> Isolated yield.

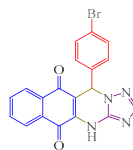
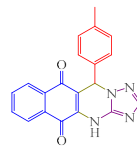
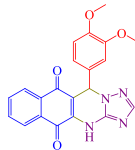
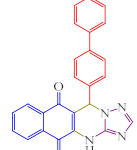
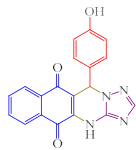
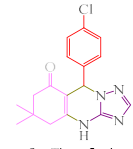
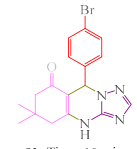
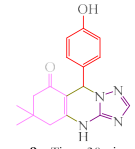
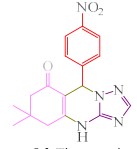
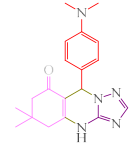
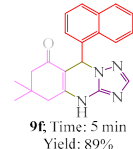
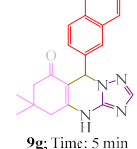
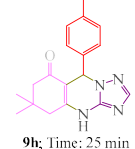
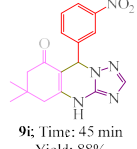
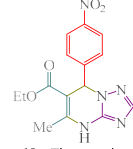
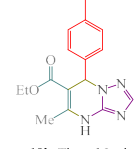
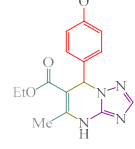
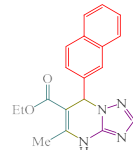
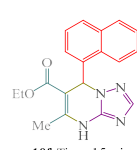
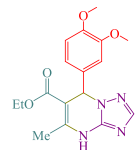
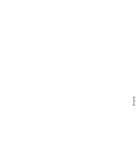
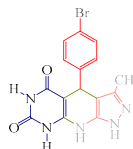
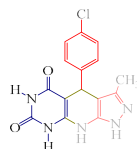
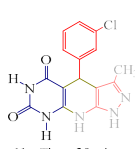
### 2.3. General procedure for synthesis of products 8–11

A mixture of aldehyde (1.0 mmol), 3-amino-1,2,4-triazole (1.0

mmol, 0.084 g, 0.014 mL), 2-hydroxy-1,4-naphthoquinone (1.0 mmol, 0.174 g, for synthesis of **8**) or dimedone (1.0 mmol, 0.140 g, for synthesis of **9**) or ethyl acetoacetate (1 mmol, 0.130 g, 0.008 mL, for

**Table 3**

Synthesis of [1,2,4]triazolo[5,1-*b*]quinazolines (**8** and **9**) and [1,2,4]triazolo[1,5-*b*]pyrimidines (**10** and **11**) using [Ni(TPPAH)][C(NO<sub>2</sub>)<sub>3</sub>]<sub>4</sub> (10 mg) under solvent-free conditions at 80 °C.<sup>a,b</sup>

 <p><b>8a</b>; Time: 5 min Yield: 95% M.p.: 320-322 °C Red solid</p>	 <p><b>8b</b>; Time: 5 min Yield: 91% M.p.: 310-311 °C Red solid</p>	 <p><b>8c</b>; Time: 15 min Yield: 95% M.p.: 287-288 °C Red solid</p>	 <p><b>8d</b>; Time: 5 min Yield: 93% M.p.: 305-308 °C Red solid</p>	 <p><b>8e</b>; Time: 5 min Yield: 95% M.p.: 275-277 °C Red solid</p>
 <p><b>9a</b>; Time: 5 min Yield: 89% M.p.: 304-305 °C Yellow solid</p>	 <p><b>9b</b>; Time: 10 min Yield: 94% M.p.: 287-288 °C Yellow solid</p>	 <p><b>9c</b>; Time: 30 min Yield: 90% M.p.: 300-301 °C Yellow solid</p>	 <p><b>9d</b>; Time: 5 min Yield: 87% M.p.: 300-301 °C Yellow solid</p>	 <p><b>9e</b>; Time: 45 min Yield: 77% M.p.: 292-293 °C Yellow solid</p>
 <p><b>9f</b>; Time: 5 min Yield: 89% M.p.: 320-321 °C Yellow solid</p>	 <p><b>9g</b>; Time: 5 min Yield: 91% M.p.: 286-287 °C Yellow solid</p>	 <p><b>9h</b>; Time: 25 min Yield: 93% M.p.: 300-301 °C Yellow solid</p>	 <p><b>9i</b>; Time: 45 min Yield: 88% M.p.: 270-271 °C Yellow solid</p>	 <p><b>9j</b>; Time: 90 min Yield: 55% M.p.: 278-279 °C Yellow solid</p>
 <p><b>10a</b>; Time: 5 min Yield: 94% M.p.: 262-264 °C Yellow solid</p>	 <p><b>10b</b>; Time: 16 min Yield: 71% M.p.: 241-243 °C White solid</p>	 <p><b>10c</b>; Time: 34 min Yield: 57% M.p.: 230-232 °C Yellow solid</p>	 <p><b>10d</b>; Time: 10 min Yield: 87% M.p.: 255-257 °C Yellow solid</p>	
 <p><b>10e</b>; Time: 45 min Yield: 69% M.p.: 235-236 °C White solid</p>	 <p><b>10f</b>; Time: 15 min Yield: 94% M.p.: 270-271 °C White solid</p>	 <p><b>10g</b>; Time: 60 min Yield: 80% M.p.: 192-193 °C White solid</p>	 <p><b>10h</b>; Time: 35 min Yield: 58% M.p.: 220-221 °C Yellow solid</p>	
 <p><b>11a</b>; Time: 30 min Yield: 73% M.p.: 305-307 °C White solid</p>	 <p><b>11b</b>; Time: 30 min Yield: 66% M.p.: 298-299 °C White solid</p>	 <p><b>11c</b>; Time: 30 min Yield: 57% M.p.: 301-303 °C Yellow solid</p>	 <p><b>11d</b>; Time: 60 min Yield: 68% M.p.: 310-312 °C Yellow solid</p>	 <p><b>11e</b>; Time: 60 min Yield: 63% M.p.: 298-299 °C Yellow solid</p>

a Reaction conditions: synthesis of **8**, aldehyde (1.0 mmol), 3-amino-1,2,4-triazole (1.0 mmol, 0.084 g, 0.014 mL), 2-hydroxy-1,4-naphthoquinone (1.0 mmol; 0.174 g); synthesis of **9**, aldehyde (1.0 mmol), 3-amino-1,2,4-triazole (1.0 mmol, 0.084 g, 0.014 mL), dimedone (1.0 mmol, 0.140 g); synthesis of **10**, aldehyde (1.0 mmol), 3-amino-1,2,4-triazole (1.0 mmol, 0.084 g, 0.014 mL), ethyl acetoacetate (1.0 mmol, 0.130 g, 0.008 mL); synthesis of **11**, aldehyde (1.0 mmol), 3-methyl-1H-pyrazol-5-amine (1 mmol, 0.097 g), pyrimidine-2,4,6(1H,3H,5H)-trione (1.0 mmol, 0.128 g, for synthesis of **11a-c**) or 1,3-dimethylpyrimidine-2,4,6(1H,3H,5H)-trione (1.0 mmol, 0.156 g, for synthesis of **11d** and **e**); b Isolated yield.

synthesis of **10** under solvent-free conditions was stirred at 80 °C using [Ni(TPPAH)][C(NO<sub>2</sub>)<sub>3</sub>]<sub>4</sub> (10 mg) as a catalyst. Also, in other work, a mixture of aldehyde (1.0 mmol), 3-methyl-1H-pyrazol-5-amine (1 mmol, 0.097 g) and pyrimidine-2,4,6(1H,3H,5H)-trione (1.0 mmol,

0.128 g, for synthesis of **11a-c**) or 1,3-dimethylpyrimidine-2,4,6(1H,3H,5H)-trione (1.0 mmol, 0.156 g, for synthesis of **11d** and **e**) was stirred under similar conditions. After the end of the reaction, observed using thin layer chromatography (TLC; *n*-hexane/ethyl acetate: 1/1), the

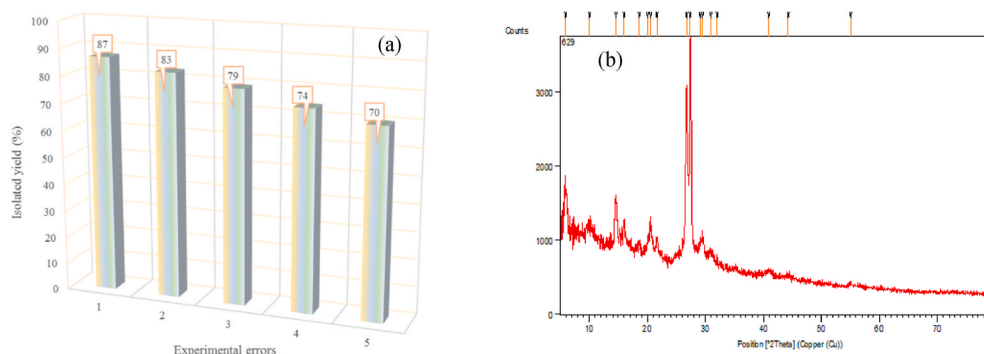


Fig. 7. (a) Recyclability study of  $[\text{Ni}(\text{TPPAH})][\text{C}(\text{NO}_2)_3]_4$  in synthesis of **10d** after 10 min and (b) XRD pattern of  $[\text{Ni}(\text{TPPAH})][\text{C}(\text{NO}_2)_3]_4$  after four consecutive runs.

Table 4

Elemental analysis of recycled  $[\text{Ni}(\text{TPPAH})][\text{C}(\text{NO}_2)_3]_4$ .

Element		C	H	N
Wt.%	Experimental	32.10	1.73	27.95
	Computational	31.68	1.50	27.71

solid mass precipitate was filtered off and washed with ethanol to separate the catalyst from other materials (the catalyst was insoluble in ethanol and the reaction mixture was soluble). The solvent of the filtrate was evaporated and the crude product was recrystallized from ethanol to give the corresponding products **8–11**. The analytical data and spectral images for compounds are presented in the Supporting Information.

### 3. Results and discussion

#### 3.1. Characterization of $[\text{Ni}(\text{TPPAH})][\text{C}(\text{NO}_2)_3]_4$

The  $[\text{Ni}(\text{TPPA})]$  was produced *via* the process of Yokote et al. [33], in the reaction of urea, 2,3-pyridine-dicarboxylic acid,  $(\text{NH}_4)_6\text{Mo}_7\text{O}_{24}\cdot 4\text{H}_2\text{O}$  and  $\text{NiCl}_2\cdot 6\text{H}_2\text{O}$ . In the next step,  $[\text{Ni}(\text{TPPA})][\text{C}(\text{NO}_2)_3]_4$  was formed using reaction between  $[\text{Ni}(\text{TPPA})]$  and trinitromethane in ethanol-acetonitrile (1:1) under reflux conditions. Finally, the morphology and structure of novel  $[\text{Ni}(\text{TPPAH})][\text{C}(\text{NO}_2)_3]_4$  were studied using several techniques: UV–Vis, FT-IR, thermal gravimetric analysis (TGA), differential thermal analysis (DTA), inductively coupled plasma (ICP) spectroscopy, CHN analysis, diffuse reflectance spectroscopy (DRS), energy-dispersive X-ray spectroscopy (EDX), scanning electron microscopy (SEM)-coupled EDX (SEM mapping), X-ray diffraction (XRD), field emission (FE)-SEM and transmission electron microscopy (TEM). The lone-pair electrons of the non-coordinated nitrogens of the catalyst precursor are orthogonal to ring p-orbitals which participate in aromaticity and are coordinated to the central metal (Ni). Therefore, these non-coordinated lone pairs are completely concentrated and localized at their corresponding nitrogens. Thus, these nitrogens have more basic ability than others. The acidic protons of trinitromethane connect to two near non-coordinated nitrogen lone pairs of the catalyst structure via hydrogen bonding (driving force of hydrogen bonding via formation of 5-membered ring).

**UV–Vis analysis:** The UV–Vis spectrum of the  $[\text{Ni}(\text{TPPAH})][\text{C}(\text{NO}_2)_3]_4$  in DMSO displays a strong Q-band at 631 nm (Fig. 1b), compared with  $[\text{Ni}(\text{TPPA})]$  which shows a strong Q-band at 627 nm (Fig. 1a). Also the visible absorption spectra display a vibration satellite at 572 nm – compared with  $[\text{Ni}(\text{TPPA})]$  which displays a vibration satellite at 569 nm – and this band is characteristic for Pc derivatives and the blue shift of the Q-band corresponding to Pcs is typical of pyridinoporphyrazine complexes [34]. Additionally, the characteristic band at the 374 nm region (B or Soret band) relates to  $\pi \rightarrow \pi^*$  transition

from the monocyclic ring in the  $[\text{Ni}(\text{TPPAH})][\text{C}(\text{NO}_2)_3]_4$ , compared with  $[\text{Ni}(\text{TPPA})]$  which shows B or Soret band at 368 nm [35,36]. The optical band-gap energy ( $E_{\text{bg}} = 1240/\lambda_{\text{max}}$ ) for  $[\text{Ni}(\text{TPPAH})][\text{C}(\text{NO}_2)_3]_4$  is 1.98 eV.

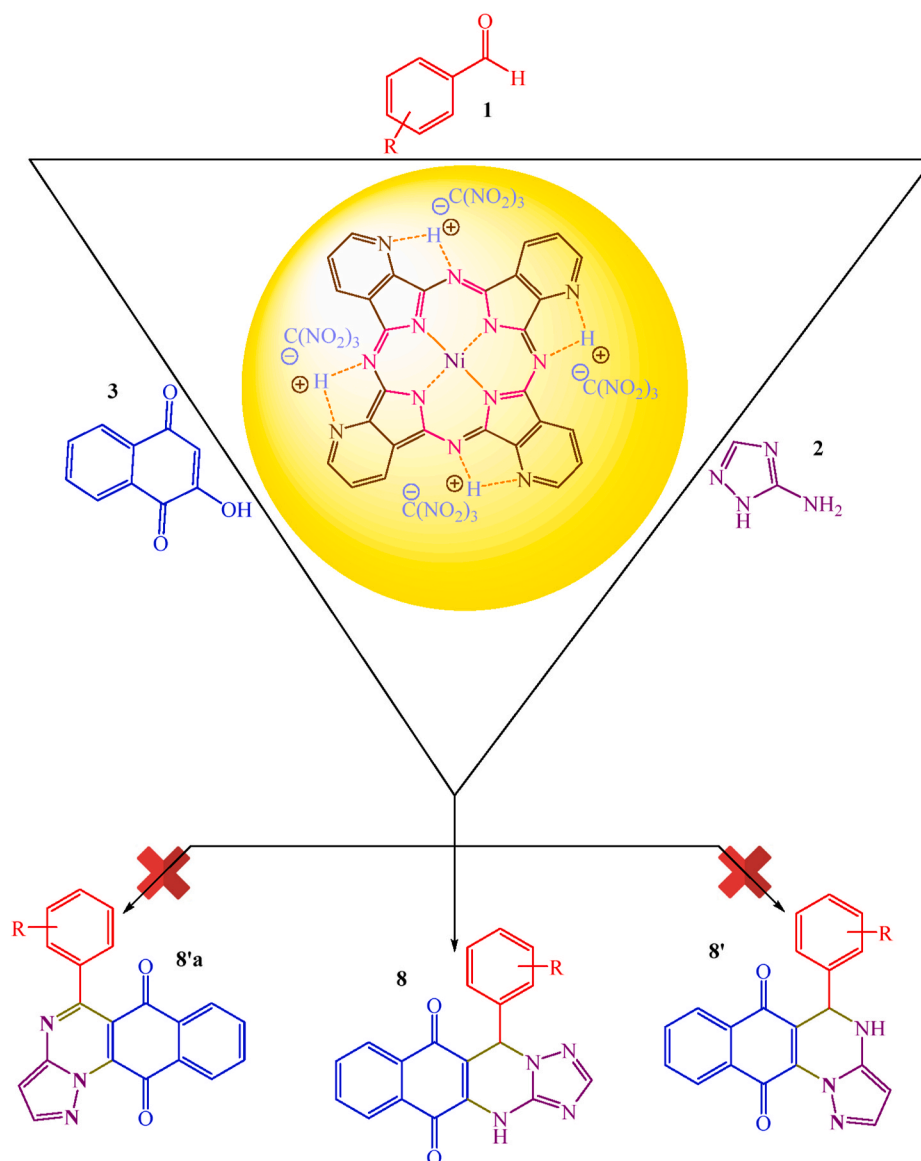
**FT-IR analysis:** The FT-IR analysis of  $[\text{Ni}(\text{TPPAH})][\text{C}(\text{NO}_2)_3]_4$  is achieved in the range of 400–4000  $\text{cm}^{-1}$  (Fig. 2). The FT-IR spectrum shows the functional groups that exist in this compound. The broad peaks around 3209 and 3070  $\text{cm}^{-1}$  are assigned to the stretching vibrations of N–H and aromatic C–H bands, respectively (the broad peaks at 3387 and 3064  $\text{cm}^{-1}$  are related to stretching vibrations of O–H in surface and aromatic C–H bands in  $[\text{Ni}(\text{TPPA})]$ , respectively). The sharp peaks at 1531 and 1345  $\text{cm}^{-1}$  can be attributed to the stretching vibrational modes of  $-\text{NO}_2$ . Remarkably, the peak at 761  $\text{cm}^{-1}$  is connected to Ni–ligand coordination bonds (the peak at 738  $\text{cm}^{-1}$  is linked to formation of Ni–ligand coordination bonds).

**TGA and DTA:** The TGA is applied for determination of thermal stability of  $[\text{Ni}(\text{TPPAH})][\text{C}(\text{NO}_2)_3]_4$  up to 600 °C (Fig. 3). These analyses show about 2% weight loss around 25–100 °C that can be ascribed to elimination of the adsorbed water and other physically adsorbed solvents remaining from the extraction procedure. The second weight loss (about 14%) at 240–325 °C is because of removal of the trinitromethanide group after the extraction procedure. Lastly, the chief weight loss (about 17%) in the range of 325–430 °C is ascribed to decomposition of the nickel tetra-2,3-pyridiniumporphyrizinato group. The TGA and DTA curves show that this compound is stable up to 430 °C. At temperatures above 430 °C, the structure of the catalyst is not stable and is destroyed.

**ICP and CHN analysis:** The exact percentage of Ni in  $[\text{Ni}(\text{TPPAH})][\text{C}(\text{NO}_2)_3]_4$  is 3.45 wt% according to the ICP result. The CHN analysis of  $[\text{Ni}(\text{TPPAH})][\text{C}(\text{NO}_2)_3]_4$  is summarized in Table 1. The CHN data of  $[\text{Ni}(\text{TPPA})]$  and  $[\text{Ni}(\text{TPPAH})][\text{C}(\text{NO}_2)_3]_4$  are shown in Figs. S43 and S44.

**DRS analysis:** The DRS and Kubelka–Munk function (derived from DRS) of  $[\text{Ni}(\text{TPPAH})][\text{C}(\text{NO}_2)_3]_4$  are investigated (Fig. 4). The main peaks in the range 300–400 nm show the transition between valence band and conduction band. The weak absorption in the UV–Vis region is probably due to transitions including outer states; for example surface traps, deficiency states, or impurity. The Kubelka–Munk theory is applied to describe the energy band gap of the  $[\text{Ni}(\text{TPPAH})][\text{C}(\text{NO}_2)_3]_4$  produced from DRS. The measured band gap energy for  $[\text{Ni}(\text{TPPAH})][\text{C}(\text{NO}_2)_3]_4$  is 1.98 eV (based on UV–Vis spectrum). The broad band at around 569 nm is due to the electronic ligand–field transition of  $\text{Ni}^{2+}$  in tetrahedral coordination [37–39].

**EDX analysis and SEM mapping:** The homogeneous and corresponding signals of the elements C, N, Ni and O are clearly shown in the EDX elemental mapping (Fig. 5), additionally confirming that the trinitromethanide molecules are attached on the  $[\text{Ni}(\text{TPPA})]$  surface by close interface exchange. As predictable, C is the chief element for all materials, with average contents about 61.7 wt%. This analysis shows average contents of 14.9 wt% N, 12.5 wt% Ni and 10.9 wt% O.



**Scheme 3.** The predicted structures of reaction adduct.

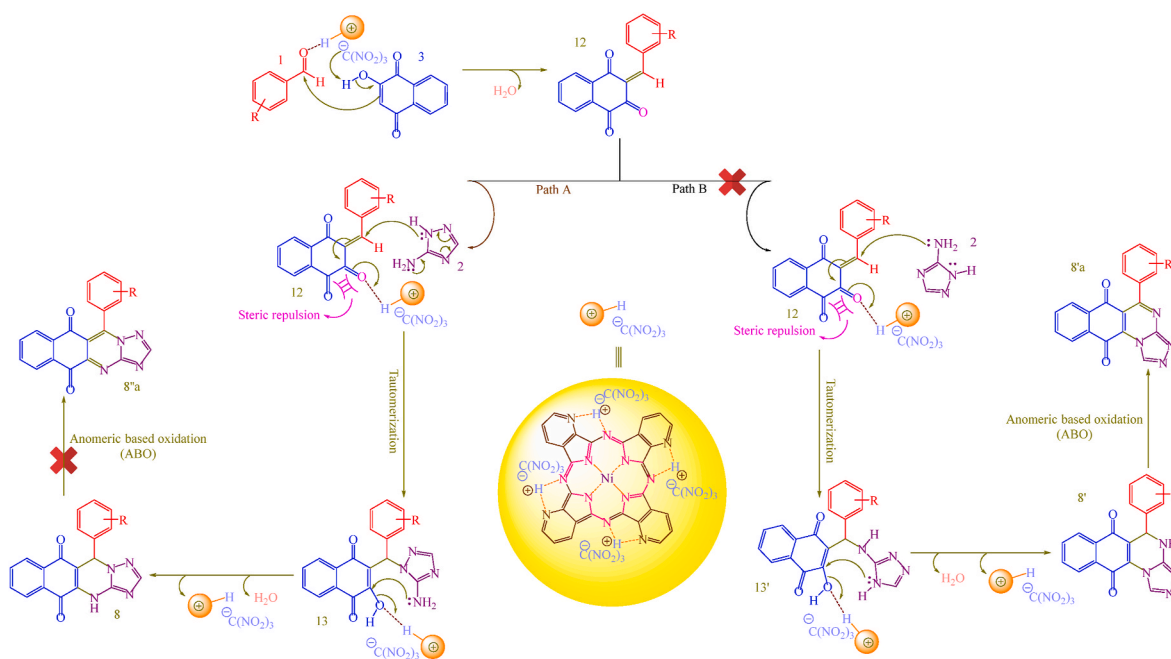
**XRD, FE-SEM and TEM analyses:** The high dispersion of [Ni(TPPAH)][C(NO<sub>2</sub>)<sub>3</sub>]<sub>4</sub> is shown by the XRD pattern of the combined materials with special peaks for Ni (Fig. 6a). The XRD pattern of this compound presents a broad maximum with the amorphous peak at  $2\theta = 27.4$ . The morphology of this compound is investigated using TEM (Fig. 6b) and SEM (Fig. 6c and d) analyses. The TEM image of this compound is in appropriate agreement with XRD analysis and confirms organized rod-like channels with high uniformity for the material. Furthermore, the surface morphology of the [Ni(TPPAH)][C(NO<sub>2</sub>)<sub>3</sub>]<sub>4</sub> is investigated by SEM imaging. This clearly shows particles with spherical morphology for the material. The particle size distribution has an average diameter of above 100 nm (XRD data of [Ni(TPPAH)][C(NO<sub>2</sub>)<sub>3</sub>]<sub>4</sub> seen in Fig. S40).

### 3.2. Catalytic application of [Ni(TPPAH)][C(NO<sub>2</sub>)<sub>3</sub>]<sub>4</sub> in synthesis of [1,2,4]triazolo[5,1-*b*]quinazolines and [1,2,4]triazolo[1,5-*b*]pyrimidines

The [Ni(TPPAH)][C(NO<sub>2</sub>)<sub>3</sub>]<sub>4</sub> (10 mg) catalyzes synthesis of [1,2,4]triazolo[5,1-*b*]quinazolines and [1,2,4]triazolo[1,5-*b*]pyrimidines from the reaction between aldehydes 1,3-amino-1,2,4-triazole, 2,2-hydroxy-1,4-naphthoquinone **3** or dimedone **4** (for synthesis of [1,2,4]triazolo

[5,1-*b*]quinazolines **8** and **9**) and ethyl acetoacetate **5** (for synthesis of [1,2,4]triazolo[1,5-*b*]pyrimidines **10**) under solvent-free conditions at 80 °C. Also, in other work, the reactions between aldehyde **1**, pyrimidine-2,4,6(1*H*,3*H*,5*H*)-trione **6a** or 1,3-dimethylpyrimidine-2,4,6(1*H*,3*H*,5*H*)-trione **6b** and 3-methyl-1*H*-pyrazol-5-amine **7** for the synthesis of [1,2,4]triazolo[1,5-*b*]pyrimidines **11** by using [Ni(TPPAH)][C(NO<sub>2</sub>)<sub>3</sub>]<sub>4</sub> as a catalyst are investigated under similar conditions.

With the aim of determining the appropriate reaction conditions for synthesis of **10d**, the substrates 4-chlorobenzaldehyde, 3-amino-1,2,4-triazole and ethyl acetoacetate are stirred together under solvent-free conditions (Table 2, entry 1) individually under catalyst-free conditions at 80 °C. There is no **10d** formation even after 120 min. This demonstrates the requirement of [Ni(TPPAH)][C(NO<sub>2</sub>)<sub>3</sub>]<sub>4</sub> as a catalyst in synthesis of **10d**. At that point a similar reaction is carried out with 10 mg of catalyst in several solvents and solvent-free conditions (Table 2, entries 2–9). The **10d** is synthesized under the related conditions and yield of the reaction is considered. From the above optimization, it is obvious a solvent-free conditions is appropriate for synthesis of **10d**. The similar reaction is also checked with other amounts of catalyst under solvent-free conditions at 80 °C (Table 2, entries 10–12). The appropriate amount of catalyst for synthesis of **10d** is 10 mg (this may be due



**Scheme 4.** Plausible mechanism for synthesis of [1,2,4]triazolo[5,1-*b*]quinazolines **8** using [Ni(TPPAH)][C(NO<sub>2</sub>)<sub>3</sub>]<sub>4</sub> as a catalyst.

to the presence of various active acidic sites in the structure of the catalyst, the functional groups of the reactants including 4-chlorobenzaldehyde, 3-amino-1,2,4-triazole and ethyl acetoacetate are protonated and inactivated. As a result, the reaction progresses to the formation of a by-product and the isolated yield of the major product decreases). Later with the optimization of solvent and catalytic amounts, the reaction temperature is also optimized. To determine the optimum temperature, reactions are carried out at various temperatures and yields of **10d** are obtained (Table 2, entries 13–15). From these descriptions, the optimum temperature for this process is established to be 80 °C.

To determine the substrate scope of this catalytic process, numerous aldehydes possessing electron-withdrawing and electron-donating groups are applied (Table 3). All of them provide suitable yields, which show the substrate scope in addition to the functional group tolerance of this process. Aldehydes possessing electron-withdrawing groups produce reasonably higher yields than those of electron-donating ones.

In this part of our investigation, the catalyst can be recovered and reused in up to four successive runs. To assess the recyclability of [Ni(TPPAH)][C(NO<sub>2</sub>)<sub>3</sub>]<sub>4</sub>, the reaction of 4-chlorobenzaldehyde, 3-amino-1,2,4-triazole and ethyl acetoacetate under solvent-free conditions at 80 °C is also studied. After the end of reaction determined using TLC, the catalyst is recovered by filtration and thoroughly washed with ethanol. Then it is dried in the oven and applied for the next runs. Fig. 7a links the difference of related product yield with the number of runs. The reusability illustration shows that the catalyst can be reused in up to four consecutive runs without decrease in yield of the related product. The exact percentage of Ni in recycled [Ni(TPPAH)][C(NO<sub>2</sub>)<sub>3</sub>]<sub>4</sub> is known to be 3.01 wt% based on the ICP result. Elemental analysis from the obtained [Ni(TPPAH)][C(NO<sub>2</sub>)<sub>3</sub>]<sub>4</sub> after its reuse is also investigated. The CHN analysis results are summarized in Table 4. The XRD pattern of [Ni(TPPAH)][C(NO<sub>2</sub>)<sub>3</sub>]<sub>4</sub> after four successive runs confirms the stability of its structure in the course of the recycling process (Fig. 7b). Moreover, the XRD patterns of [Ni(TPPAH)][C(NO<sub>2</sub>)<sub>3</sub>]<sub>4</sub> (before and after recycling) show the stability of described catalyst structure (XRD data of recycled [Ni(TPPAH)][C(NO<sub>2</sub>)<sub>3</sub>]<sub>4</sub> is presented in Fig. S41). Elemental analysis data of [Ni(TPPAH)][C(NO<sub>2</sub>)<sub>3</sub>]<sub>4</sub> are shown in Fig. S45. The reaction is scaled up to 10 mmol of 4-chlorobenzaldehyde, 3-amino-1,2,4-triazole and ethyl acetoacetate for the synthesis of **10d** in the presence of 100 mg

of [Ni(TPPAH)][C(NO<sub>2</sub>)<sub>3</sub>]<sub>4</sub> under solvent-free conditions at 80 °C. The isolated yield of the reaction is 87% after 10 min, and 70% after the fifth run.

These compounds could be puzzle pieces in our research on developing our newly established “anomeric based oxidation” mechanism [40–42]. In contrast to our expected products, the spectral data show that the reaction proceeds toward the synthesis of **8** (Scheme 3).

According to the results, a possible mechanism is suggested (Scheme 4) [22–25], in which [Ni(TPPAH)][C(NO<sub>2</sub>)<sub>3</sub>]<sub>4</sub> acts as a bifunctional catalyst. In the first step, [Ni(TPPAH)][C(NO<sub>2</sub>)<sub>3</sub>]<sub>4</sub> activates the carbonyl group of aldehyde **1** to attack the enolate form of 2-hydroxy-1,4-naphthoquinone **3**. Then, the Knoevenagel condensation between activated aldehyde **1** and enolate **3** leads to synthesis of heterodiene **12** via elimination of one molecule of water. In the next step, synthesis of intermediate **13** happens via nucleophilic attack of 3-amino-1,2,4-triazole **2** to heterodiene **12**. Intramolecular cyclization via the condensation of the amino group of **2** with 2-hydroxy-1,4-naphthoquinone **3** in the intermediate **13** via elimination of one molecule of water yields the desired product **8**. In this entire method, [Ni(TPPAH)][C(NO<sub>2</sub>)<sub>3</sub>]<sub>4</sub> is regenerated and reused for consequent reaction. The reported studies and X-ray crystallography investigations show that this mechanism proceeds via path A [22–25] and the amino group inside the ring in 3-amino-1,2,4-triazole **2** reacts with intermediate **12** and the desired product **8** is formed.

#### 4. Conclusions

The [Ni(TPPAH)][C(NO<sub>2</sub>)<sub>3</sub>]<sub>4</sub> is efficaciously employed as a novel heterogeneous catalyst for synthesis of [1,2,4]triazolo[5,1-*b*]quinazolines and [1,2,4]triazolo[1,5-*b*]pyrimidines from reactants aldehyde, 3-amino-1,2,4-triazole, 2-hydroxy-1,4-naphthoquinone or dimedone or ethyl acetoacetate under benign reaction conditions. Also, in other study, the reaction between aldehydes, 3-methyl-1*H*-pyrazol-5-amine and pyrimidine-2,4,6(1*H*,3*H*,5*H*)-trione or 1,3-dimethylpyrimidine-2,4,6(1*H*,3*H*,5*H*)-trione for synthesis of [1,2,4]triazolo[1,5-*b*]pyrimidines is investigated under similar conditions in the presence of [Ni(TPPAH)][C(NO<sub>2</sub>)<sub>3</sub>]<sub>4</sub> as a catalyst. These compounds are synthesized with good yields and appropriate functional group tolerance. The [Ni(TPPAH)][C(NO<sub>2</sub>)<sub>3</sub>]<sub>4</sub> is significant in view of its simple preparation,

physical and chemical stability, facile recyclability, environmentally friendly nature and finally accordance with some parts of green chemistry. It can therefore be applied as a heterogeneous catalyst in organic functional group transformations and should also find wide catalytic uses in industry. Some of the synthesized molecules (10 items) are reported for the first time.

### Supporting information

The Supporting Information gives general information, analytical data, spectral images of FT-IR,  $^1\text{H}$  NMR,  $^{13}\text{C}$  NMR and CHN analysis of products, XRD data of fresh and recycled catalyst, and CHN analysis data of [Ni(TPPA)] and recycled catalyst.

### Author statement

Mr. Mohammad Dashteh, Ph.D. Student of Organic Chemistry, Dr. Saeed Baghery, Ph.D. of Organic Chemistry Prof. Dr. Mohammad Ali Zolfigol, Ph.D. of Organic Chemistry, Prof. Dr. Ardeshir Khazaei, Ph.D. of Organic Chemistry, Mr. Sajjad Makhdomi, Master of Toxicology, Dr. Maliheh Safaiee, Ph.D. of Organic Chemistry, Dr. Jamshid Rakhtshah, Ph.D. of Inorganic Chemistry, Prof. Dr. Yadollah Bayat, Ph.D. of Organic Chemistry, Dr. Asiye Asgari, Ph.D. of Organic Chemistry.

### Declaration of competing interest

The authors declare no conflict of interest.

### Acknowledgments

We thank Bu-Ali Sina University and the Iran National Science Foundation (INSF) (Grant Number 98001912) for financial support to our research group.

### Appendix A. Supplementary data

Supplementary data to this article can be found online at <https://doi.org/10.1016/j.jpics.2021.110322>.

### References

- [1] L.F. Tietze, *Chem. Rev.* 96 (1996) 115–136.
- [2] A. Dömling, I. Ugi, *Angew. Chem. Int. Ed.* 39 (2000) 3168–3210.
- [3] A. Dömling, *Chem. Rev.* 106 (2006) 17–89.
- [4] J. Zhu, H. Bienaymé, *Multicomponent Reactions*, Wiley-VCH, Weinheim, Germany, 2005, pp. 33–75.
- [5] K.C. Nicolaou, D.J. Edmonds, P.G. Bulger, *Angew. Chem. Int. Ed.* 45 (2006) 7134–7186.
- [6] B.B. Toure, D.G. Hall, *Chem. Rev.* 109 (2009) 4439–4486.
- [7] V. Alagarsamy, V.R. Solomon, M. Murugan, *Bioorg. Med. Chem.* 15 (2007) 4009–4015.
- [8] V. Alagarsamy, *Pharmazie* 59 (2004) 753–755.
- [9] V. Alagarsamy, G. Murugananthan, R. Venkateshperumal, *Biol. Pharm. Bull.* 26 (2003) 1711–1714.
- [10] M.-J. Hour, L.-J. Huang, S.-C. Kuo, Y. Xia, K. Bastow, Y. Nakanishi, E. Hamel, K.-H. Lee, *J. Med. Chem.* 43 (2000) 4479–4487.
- [11] V. Alagarsamy, R. Revathi, S. Meena, K.V. Ramaseshu, S. Rajasekaran, E. De Clercq, *Indian J. Pharmaceut. Sci.* 66 (2004) 459–462.
- [12] K.-C. Liu, M.-K. Hu, *Arch. Pharm.* 319 (1986) 188–189.
- [13] V. Haridas, K. Lal, Y.K. Sharma, *Tetrahedron Lett.* 48 (2007) 4719–4722.
- [14] X.-Y. Sun, C. Hu, X.-Q. Deng, C.-X. Wei, Z.-G. Sun, Z.-S. Quan, *Eur. J. Med. Chem.* 45 (2010) 4807–4812.
- [15] R. Magan, C. Marin, M.J. Rosales, J.M. Salas, M. Sanchez-Moreno, *Pharmacology* 73 (2005) 41–48.
- [16] X.-Q. Deng, L.-N. Quan, M.-X. Song, C.-X. Wei, Z.-S. Quan, *Eur. J. Med. Chem.* 46 (2011) 2955–2963.
- [17] R. Magan, C. Marin, J.M. Salas, M.B. Perez, M.J. Rosales, M.I. Men Instaswaldo Cruz, *Rio de Janeiro* 99 (2004) 651–656.
- [18] R.P. Brigance, W. Meng, A. Fura, T. Harrity, A. Wang, R. Zahler, M.S. Kirby, L. G. Hamann, *Bioorg. Med. Chem. Lett.* 20 (2010) 4395–4398.
- [19] J.A.R. Navarro, J.M. Salas, M.A. Romero, R. Vilaplana, F. Gonzalez-Vilchez, R. Faure, *J. Med. Chem.* 41 (1998) 332–338.
- [20] W. Yu, C. Goddard, E. Clearfield, C. Mills, T. Xiao, H. Guo, J.D. Morrey, N. E. Motter, K. Zhao, T.M. Block, A. Cucconati, X. Xu, *J. Med. Chem.* 54 (2011) 5660–5670.
- [21] V.L. Rusinov, A.Yu Petrov, T.L. Pilicheva, O.N. Chupakhin, G.V. Kovalev, E. R. Komina, *Pharm. Chem. J.* 20 (1986) 113–117.
- [22] W. Li, S. Tian, L. Wu, *Bull. Kor. Chem. Soc.* 34 (2013) 2825–2828.
- [23] L. Wu, C. Zhang, W. Li, *Bioorg. Med. Chem. Lett.* 23 (2013) 5002–5005.
- [24] R. Sompalle, S.M. Roopan, N.A. Al-Dhabi, K. Suthindhiran, G. Sarkar, M.V. Arasu, *J. Photochem. Photobiol., B* 162 (2016) 232–239.
- [25] M. Kidwai, R. Chauhan, *J. Mol. Catal. Chem.* 377 (2013) 1–6.
- [26] P.R. Ortiz de Montellano (Ed.), *Cytochrome P-450: Structure, Mechanism and Biochemistry*, second ed., Plenum Press, New York, 1995.
- [27] K.M. Kadish, K.M. Smith, R. Guilard (Eds.), *The Porphyrin Handbook*, vol. 6, Academic Press, San Diego, 2003.
- [28] K.M. Kadish, K.M. Smith, R. Guilard (Eds.), *Handbook of Porphyrin Science*, vols. 1–35, World Scientific Publishing Co., Singapore, 2014.
- [29] E. Ben-Hur, W.-S. Chan, *Phthalocyanines in photobiology and their medical applications*, in: K.M. Kadish, K.M. Smith, R. Guilard (Eds.), *The Porphyrin Handbook: Applications of Phthalocyanines*, vol. 19, Academic Press, USA, 2012, <https://doi.org/10.1016/B978-0-08-092393-2.50007-X>.
- [30] (a) F. Dumoulin, M. Durmuş, V. Ahsen, T. Nyokong, *Coord. Chem. Rev.* 254 (2010) 2792–2847; (b) A.B. Sorokin, *Chem. Rev.* 113 (2013) 8152–8191; (c) H. Lu, N. Kobayashi, *Chem. Rev.* 116 (2016) 6184–6261; (d) C.G. Claessens, U. Hahn, T. Torres, *Chem. Rec.* 8 (2008) 75–97.
- [31] (a) M. Dashteh, M. Safaiee, S. Baghery, M.A. Zolfigol, *Appl. Organomet. Chem.* 33 (4) (2019), e4690, 1–14; (b) S. Baghery, M.A. Zolfigol, M. Safaiee, D.A. Alonso, A. Khoshnood, *Appl. Organomet. Chem.* 31 (1–14) (2017) e3775.
- [32] (a) M. Safaiee, M.A. Zolfigol, F. Afsharnadery, S. Baghery, *RSC Adv.* 5 (2015) 102340–102349; (b) M.A. Zolfigol, M. Safaiee, N. Bahrami-Nejad, *New J. Chem.* 40 (2016) 5071–5079; (c) M.A. Zolfigol, M. Safaiee, N. Bahrami-Nejad, *New J. Chem.* 40 (2016) 8158–8160; (d) M. Safaiee, M. Moeinimehr, M.A. Zolfigol, *Polyhedron* 170 (2019) 138–150.
- [33] (a) M. Yokote, F. Shibamiya, S. Tokairin, *Kogyo Kagaku Zasshi*, 166, *Chem. Abstr.* 61 (1964) (1964) 67, 3235f; (b) T.D. Smith, J. Livorness, H. Taylor, *J. Chem. Soc. Dalton Trans.* (1983) 1391–1400; (c) I. Seotsanyana-Mokhosi, N. Kuznetsova, T. Nyokong, *J. Photochem. Photobiol. Chem.* 140 (2001) 215–222.
- [34] D. Wöhrle, J. Gitzel, I. Okura, S. Aono, *J. Chem. Soc., Perkin Trans. II* (1985) 1171–1175.
- [35] C.C. Leznoff, A.B.P. Lever, *Phthalocyanines and Applications*, Wiley-VCH, 1989.
- [36] A.J. Jeevagan, S.A. John, *RSC Adv.* 3 (2013) 2256–2264.
- [37] M. Srinivas, T.O.S. Kumar, K.M. Mahadevan, G.R. Vijayakumar, H. Nagabhushana, M.N. Kumara, S. Naveen, N.K. Lokanath, *J. Sci. Adv. Mater. Dev.* 1 (2016) 324–329.
- [38] J.-L. Ortiz-Quinonez, U. Pal, M.S. Villanueva, *ACS Omega* 3 (2018) 14986–15001.
- [39] S.A. Kahani, F. Abdevali, *RSC Adv.* 6 (2016) 5116–5122.
- [40] P. Ghasemi, M. Yarie, M.A. Zolfigol, A. Taherpour, *ACS Omega* 5 (2020) 3207–3217.
- [41] M. Yarie, *Iran. J. Catal.* 7 (2017) 85–88.
- [42] M. Yarie, *Iran. J. Catal.* 10 (2020) 79–83.